**Title**

# Listener-based Analysis of Surface Importance for Acoustic Metrics



**Authors**
Michel, Frank
Deines, Eduard
Bertram, Martin
et al.

**Publication Date**
2007

Peer reviewed

# Listener-based Analysis of Surface Importance for Acoustic Metrics

Frank Michel, Eduard Deines, Martin Hering-Bertram, Christoph Garth and Hans Hagen *Member, IEEE*

**Abstract**—Acoustic quality in room acoustics is measured by well defined quantities, like definition, which can be derived from simulated impulse response filters or measured values. These take into account the intensity and phase shift of multiple reflections due to a wave front emanating from a sound source. Definition ($D_{50}$) and clarity ($C_{50}$) for example correspond to the fraction of the energy received in total to the energy received in the first 50 ms at a certain listener position. Unfortunately, the impulse response measured at a single point does not provide any information about the direction of reflections, and about the reflection surfaces which contribute to this measure. For the visualization of room acoustics, however, this information is very useful since it allows to discover regions with high contribution and provides insight into the influence of all reflecting surfaces to the quality measure.
We use the phonon tracing method to calculate the contribution of the reflection surfaces to the impulse response for different listener positions. This data is used to compute importance values for the geometry taking a certain acoustic metric into account. To get a visual insight into the directional aspect, we map the importance to the reflecting surfaces of the geometry. This visualization indicates which parts of the surfaces need to be changed to enhance the chosen acoustic quality measure.
We apply our method to the acoustic improvement of a lecture hall by means of enhancing the overall speech comprehensibility (clarity) and evaluate the results using glyphs to visualize the clarity ($C_{50}$) values at listener positions throughout the room.

**Index Terms**—Sound analytics, Applications of Visualization, Room Acoustics, Phonon Tracing, Acoustic Metric

## 1 Introduction

The interplay between acoustic material properties and reflection surface geometry is one of the most interesting phenomena in the simulation and exploration of room acoustics. When analyzing the properties of existing congress and concert rooms, it may be possible to obtain a certain improvement by the choice of materials, such as carpet and paneling, whereas the geometry may not be subject to change in a greater scale. Therefore, it is important to understand the acoustic phenomena in advance and to integrate acoustic simulations into the planning phase, in the same way as this is already practice for optical design issues.

To better understand room acoustics, a variety of simulation techniques, such as finite element methods, image-source methods, and ray tracing have been employed. There are certain similarities between sound and light, allowing the adaption of many techniques developed for rendering to the scope of acoustics. For example, the combination of diffuse and specular reflection components can be defined in general by a bi-directional reflection-distribution function (BRDF), denoting the probability for incoming energy flux from a certain direction to be reflected into another direction. The acoustic equivalent are reflection (one minus absorption) and scattering coefficients which are also frequency dependent. In contrast to light where only three frequency bands need to be distinguished, acoustic absorption functions are usually spread into at least ten and up to thirty frequency bands. Due to the greater wave lengths of sound, the typical reflections are much more specular, compared to light.

For the assessment of acoustic room quality, we make the assumption of a fixed-point sound source, which can be extended to a (small) set of sources or to a regional source with prescribed emission distribution. In many cases, like demonstration rooms and theaters, the location of important sound sources is relatively constrained. For this type of application, we have previously developed a geometric approach called *phonon tracing* [5, 10], which represents the totality of directed reverberations for static sources by a set of sound particles (phonons) located on all reflecting surfaces. A recent improvement of our simulation method facilitates the reproduction of continuous pressure and energy fields with correct attenuation.

We note that there exists a variety of competing simulation approaches, like finite elements for the correct modeling of diffraction and acoustic raytracing [2] facilitating the use of moving sources. Since many of these approaches can be used in alternative to our phonon method, they are summarized in the next section among related work on acoustic visualization and auralization.

All these approaches however, simulate certain quality measures throughout a room but without identifying which parts of the room contribute to this measures and more important what needs to be changed to enhance these measures. In practice, measurements of directed sound can be performed with the aid of microphone arrays, which can be simulated easily by computing response filters at multiple points.

The core contribution of our work is a novel visualization method extending the use of previous quality measures, like clarity and clearness [1], to the scope of directed sound. Therefore we visualize the importance of scene surfaces for the quality measures at different listener positions or the complete audience. Here importance denotes how much a certain scene surface contributes to a quality measure like definition. On the basis of these visualizations one can get direct insight into which parts of the room surface need to be changed (i.e. materials) to enhance a certain quality measure.

The simulation method obtaining the underlying data and its recent implementation details are summarized in section 3. The calculation of the importance values is described in section 4. Section 5 illustrates our visualization approach, followed by results and evaluations in section 6.

## 2 Related Work

In the theory of acoustics there are two main approaches simulating the propagation of sound. The first approach is based on wave equations that are numerically solved, for example using finite element methods (FEM). The simulation results are very accurate, but the complexity increases drastically with the highest frequency considered. Hence, the wave model is suitable for low frequencies only.

The second approach, known as geometric acoustics, describes the sound propagation by sound particles moving along a directed ray.

- *Frank Michel is with IRTG Kaiserslautern, E-mail: michel@informatik.uni-kl.de.*
- *Eduard Deines is with IRTG Kaiserslautern*
- *Christoph Garth is with the University of Kaiserslautern and the Institute for Data Analysis and Visualization at the University of California in Davis.*
- *Hans Hagen is with the University of Kaiserslautern.*
- *Martin Hering-Bertram is with Fraunhofer ITWM Kaiserslautern.*

*Manuscript received 31 March 2007; accepted 1 August 2007; posted online 27 October 2007.* Published 14 September 2007.
*For information on obtaining reprints of this article, please send e-mail to: tvcg@computer.org.*

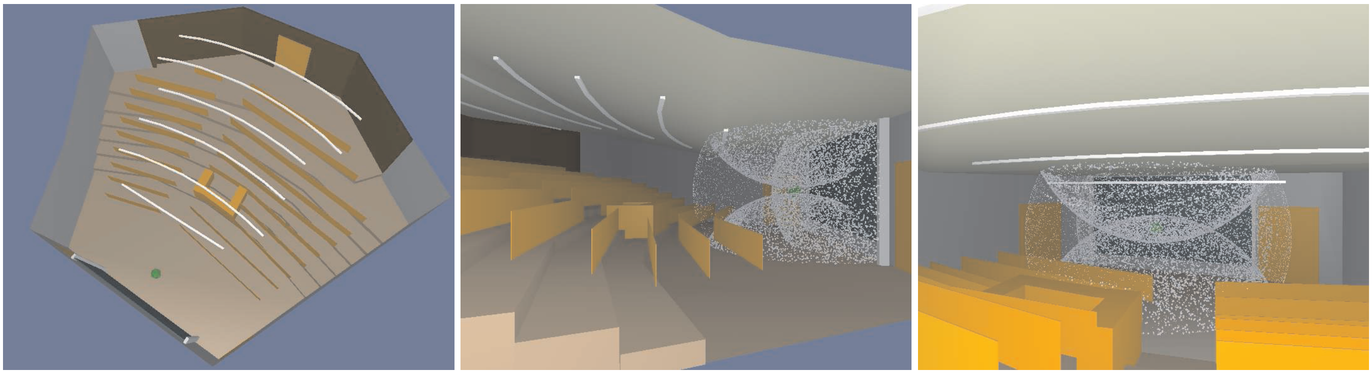

(a) (b) (c)

Fig. 1. Geometry (a) of the lecture room 46/110 and visualization (b+c) of the sound particle propagation

There exists a variety of such methods for simulating room acoustics. They are mostly based on optical fundamentals, and make use of approaches developed there. Two classical methods for acoustic simulation are the image-source method [3, 6] and the raytracing method [19, 20].

Due to the shortcomings of the two classical approaches, continuative methods have been developed in recent years. Mostly, they employ parts of the classical schemes or a combination of them. One approach that uses the advantages of the image-source method and raytracing is introduced in [26]. Here the visibility check of the image-source algorithm is performed via raytracing. In [23] a modification of the image-source method is presented, which reduces the computation demands by use of binary space partitioning. Beam-tracing methods [12, 13, 21, 25] overcome the aliasing problem of classical raytracing by recursively tracing pyramidal beams, implying the need for highly complex geometric operations. Other approaches utilizing the photon mapping [14] also exist [17], but do not address the visualization of acoustical parameters. The phonon tracing approach [5] precomputes particle traces and records the phonons direction and energy at reflecting surfaces for the collection phase. The particles contribute to the room impulse response at given listener positions. Also, approaches modeling diffraction effects have been developed in recent years [4, 15, 16].

There are a couple of objective metrics [1] for the evaluation of the acoustics inside a room. These metrics can be derived from the room impulse response and describe in most cases the ratio of early reflections to late reverberations. These properties are for example, lateral energy fraction, interaural cross correlation and early decay time. Two of the important measures for concert halls and lecture rooms are definition, determining the comprehensibility of the speech, and clarity, denoting the capability to distinguish between two consecutive tones.

The question comes up for an appropriate visual representation of the simulation results. Stettner et. al. [24] visualize room acoustic quality properties such as clarity or spatial impression using specific icons. Furthermore, they color the room boundaries according to the pressure level. Khoury et. al. [18] represent the sound pressure levels inside the room by means of color maps. Additionally, the authors analyze the precedence effect (or law of the first wavefront) by using isosurfaces. Funkhouser et. al. [12] visualize source points, receiver points, pyramidal beams, reverberation paths etc. in order to understand and evaluate their acoustic modeling method. The system also provides the presentation of acoustic measures like power and clarity. Existing commercial systems [22, 8, 7] provide some tools for visualizing the computed acoustic metrics throughout the audience, but do not show how it can be improved.

In [11] we have presented various visualization approaches for analyzing acoustic behavior inside a room utilizing the phonon map resulting from our phonon tracing algorithm [5]. Visualization of color coded phonons according to their energy spectra gave a direct insight in the material influence to the sound traversing the room. A more natural method was to visualize wavefronts propagating from the sound source. The introduced listener-based visualization allowed a time-dependent view on the received energy at distinct positions throughout the room.

## 3 Simulation Data

In this section, we describe the data used for the visualization, as well as its generation. For the simulation of the acoustics inside a room with given geometry and absorption functions at the surfaces we use the phonon tracing algorithm described in [5]. A recent improvement of this algorithm [10] uses Gaussian basis functions with approximate partition of unity to represent wave fronts. This is obtained by constructing the basis functions on the unit sphere around a sound source and dilating them with the traversed distance of the associated phonons, see figure 2. In contrast to the original approach where quadratic attenuation is used because of the spatial particle density, the improved phonon trace facilitates both linear and quadratic attenuation for the simulation of energy and pressure, respectively. This is obtained by scaling the basis functions according to the wave front propagation. Due to partition of unity, both simulated fields are continuous and smooth.

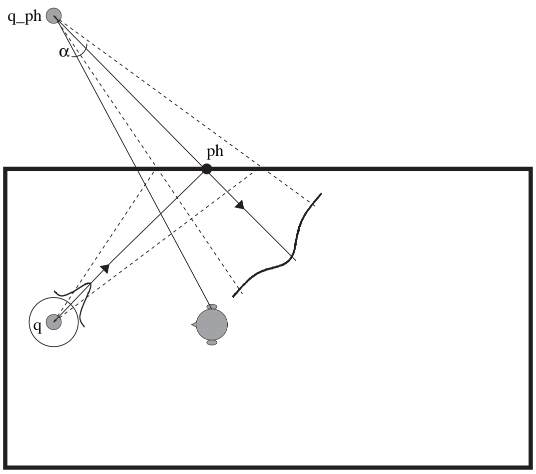


Fig. 2. Sketch of the phonon tracing algorithm to trace sound pressure inside closed rooms.

The improved phonon tracing is comprised of two steps: *Phonon emission* calculating the particle traces and storing phonons on all reflecting surfaces in a *phonon map* and the *phonon collection* step used for the calculation of impulse response filters at given listener positions. As result of the *emission step* we obtain the *phonon map* which represents all reflections of an emitted wave front by a large set of particles (phonons) which can be considered as individual micro-sources in analogy to the image-source method. For each phonon in the phonon map the following information is stored:

- a pressure or energy spectrum $p_{ph} : \Omega \mapsto \mathbf{R}^+$
- the virtual source $q_{ph}$ from which we can calculate the phonon's outgoing direction $v_{ph}$ and the traversed distance $d_{ph}$
- the phonon's current position $pt_{ph}$
- the number of reflections $r_{ph}$
- and the material index $m_{ph}$ at the current position

In order to compute the impulse response at a given listener position $l_i$ each phonon, which is visible from $l_i$, contributes to the individual frequency bands, as described in [5].
In the present work, we are not concerned with filter reconstruction, but rather with the energy and pressure amplitudes at a given listener position $l_i$. The contribution of a specific phonon to the listener position $l_i$ is denoted in equation (1) (pressure) and equation (2) (energy).

$$\begin{aligned} p_{ph}(t,l_i) &= \frac{\rho_{p,tot}\, p_0}{d_{ph}} w\Big(\angle\left(v_{ph}, l_i - q_{ph}\right)\Big) \times \delta\Big(t - \frac{d_{ph}}{c}\Big) \\ \rho_{p,tot} &= \prod \sqrt{1-\alpha_j} \qquad (1) \\ e_{ph}(t,l_i) &= \frac{\rho_{e,tot}\, e_0}{d_{ph}^2} w\Big(\angle\left(v_{ph}, l_i - q_{ph}\right)\Big) \times \delta\Big(t - \frac{d_{ph}}{c}\Big) \\ \rho_{e,tot} &= \prod (1-\alpha_j) \qquad (2) \end{aligned}$$

where $p_0$ and $e_0$ are reference pressure and energy at 1m distance from the source respectively, $\alpha_j$ are the absorption coefficients along the phonon path, $\delta(t)$ is a discrete Dirac impulse shifted by the time elapsed between emission and reception of a phonon, and $w$ is a Gaussian weighting function,

$$w(\phi) = \frac{2}{n_{ph}\sigma^2} e^{-\frac{\phi^2}{2\sigma^2}}. \qquad (3)$$

The radius $\sigma$ can be chosen such that all Gaussian basis functions approximately sum up to one on the unit sphere. We note that there is a trade off between smoothness of the partition of unity and resolution of geometric shapes that can be represented in this basis.

In the next section we describe how the simulated data is used to calculate the importance values for the reflection surfaces.

## 4 Importance Values

Our intention is to visualize which parts of the scene surface are most important for a certain acoustic measure at every listener postion $l_i$. To calculate an importance value for a phonon we use the pressure contribution of the phonon $ph_j$ to the impulse response at a given listener position $l_i$.

Because the phonon tracing method re-uses particle paths for multiple phonons (a phonon is stored at every reflection, tracing a large number of reflections until the energy contribution drops below a threshold) we have to take subsequent phonons on the same path into account when calculating the pressure contribution for a certain phonon $ph_j$ (see figure 3 (a)). Figure 3 (b) depicts one phonon paths throughout the room.

The contribution of a single phonon $ph$ to the impulse response is denoted in equations (1)(pressure) and (2)(energy). All phonons corresponding to one reflection path are listed in consecutive order within the phonon map, say $ph_{k_0}, ph_{k_0+1}, \cdots, ph_{k_n}$. The pressure and energy contribution of a phonon $ph_j$ to the impulse response at listener position $l_i$ is then the accumulated contribution of itself and its successors as stated in equation (4) for pressure $con_p$ and energy $con_e$.

$$con_p(ph_j, l_i) = \sum_{k=j}^{k_n} p_{ph_k}(t, l_i)$$

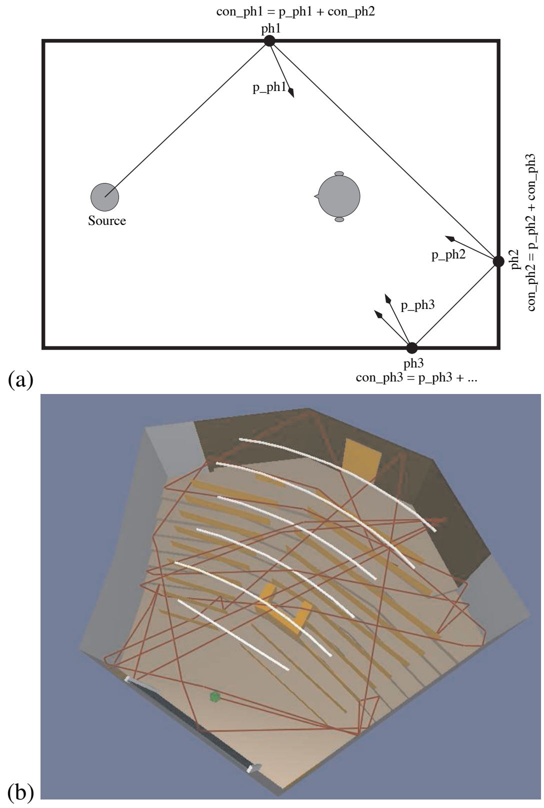


Fig. 3. (a) Calculation of the contribution $con_{ph}$ for phonons sharing the same path. (b) Illustration of one phonon path.

$$con_e(ph_j, l_i) = \sum_{k=j}^{k_n} e_{ph_k}(t, l_i), \qquad (4)$$

where $ph_j$ is the current phonon, $l_i$ the listener position and $p_{ph_k}$, $e_{ph_k}$ are the pressure and energy contribution of a phonon as in equations (1) and (2).

Due to the fact that all phonons sharing the same path are listed consecutively in the phonon map we can easily compute the contribution of a phonon by forward summation of the contribution of subsequent phonons. In addition to the importance of the phonon to one listener position $l_i$ we also calculate the contribution of the phonon to all listener positions in the scene (or to a selected subset) by:

$$\begin{aligned} con_{p\ all}(ph_j) &= \sum_{i=0}^{n_l} con_p(ph_j, l_i) \\ con_{e\ all}(ph_j) &= \sum_{i=0}^{n_l} con_e(ph_j, l_i) \qquad (5) \end{aligned}$$

where $n_l$ is the number of listeners, $con_p(ph_j, l_i)$ and $con_e(ph_j, l_i)$ are the contributions of a phonon to a single listener position $l_i$.

To calculate an importance value $imp_e(ph, l_i)$ and $imp_p(ph, l_i)$ for a phonon $ph$ and listener position $l_i$ we calculate the fraction between the contribution of the phonon $ph$ to the pressure or energy at the listener position $l_i$ and the total received pressure or energy at the listener position (i.e. percentage of pressure received at position $l_i$ from phonon $ph$).

$$\begin{aligned} imp_p(ph_j, l_i) &= \frac{con_p(ph_j, l_i)}{p_{tot,l_i}} \\ p_{tot,l_i} &= \sum_{k=0}^{n_{ph}} p_{ph_k}(t, l_i) \\ imp_e(ph_j, l_i) &= \frac{con_e(ph_j, l_i)}{e_{tot,l_i}} \end{aligned}$$

$$e_{tot,l_i} = \sum_{k=0}^{n_{ph}} e_{ph_k}(t,l_i) \quad (6)$$

where $l_i$ is the listener position, $con_p(ph_j,l_i)$ and $con_e(ph_j,l_i)$ are the contributions of phonon $ph_j$ to the listener position $l_i$, $n_{ph}$ is the total number of phonons, $p_{tot,l_i}$ and $e_{tot,l_i}$ are the total pressure and energy received at $l_i$.

To evaluate speech comprehensibility in room acoustics, for example, it is important to relate the early reflections to the later reverberations. Therefore, we provide an option to choose a time limit $t_{end}$ such that the contribution of each phonon that reaches the listener after $t_{end}$ is set to zero. By means of the importance values for each phonon in the map we provide a visualization of the impact of reflection surfaces in the scene for a chosen range of listeners. We describe our visualization approach in the following section.

## 5 Visualization

In the following we describe our visualization approach conveying the importance of particular room surfaces for the received sound signal at a listener position. The goal of the visualization is to highlight the surfaces of the scene that reflect the most energy of a sound wave to a given listener position. These surfaces are most important for the evaluation of acoustic behavior regarding acoustic measures such as definition ("Deutlichkeit" [1]) and clarity. These acoustic metrics consider the amount of early received energy to the amount of entire and late received energy respectively. Definition ("Deutlichkeit") for example is defined as:

$$D_{50} = \frac{\int_0^{50ms} p^2(t)\mathrm{d}t}{\int_0^{\infty} p^2(t)\mathrm{d}t} \quad (7)$$

From 7 we can derive the clarity metric as follows:

$$C_{50} = 10\ log\left(\frac{D_{50}}{1-D_{50}}\right) = 10\ log\left(\frac{\int_0^{50ms} p^2(t)\mathrm{d}t}{\int_{50ms}^{\infty} p^2(t)\mathrm{d}t}\right) \quad (8)$$

where $p$ is the pressure calculated or measured at the listener position. This metric is defined without regards to the direction where the sound energy came from. We provide a visualization system that allows to observe the origin of the early and entire energy, respectively, and relate them visually to each other.

First, we perform some preprocessing steps in order to prepare the scene geometry for the visualization. The 3D room models used for simulation and visualization are defined in Wavefront obj format. The scene consists of triangulated objects. After the tracing process we know the phonons' positions and connect each phonon to the reflecting scene object. The triangulation of the scene used for the acoustic simulation is low in resolution to keep the computation moderate. For a detailed visualization we need more sample points to provide the correct approximation of the surface importance. Therefore we refine the triangles by use of a subdivision algorithm as outlined in Fig. 4. We terminate the subdivision when all edges of a triangle have a smaller length than a given threshold $\lambda$.

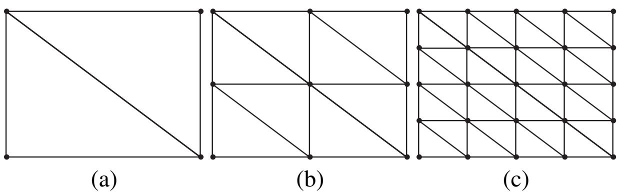


Fig. 4. Surface subdivision. (a) initial triangulated surface. (b) triangulation after first subdivision step. (c) triangulation after second subdivision step.

In order to obtain the desired level of detail for the visualization we map color values to the vertices depending on the contributions of the phonons associated with adjacent triangles. Since we have many more phonons than vertices we use a scattered data approximation approach

$$imp_{v_i} = \frac{\sum_{k=0}^{m} \omega \cdot imp(ph_k)}{\sum_{i=0}^{m} \omega}$$
$$\omega = \frac{1}{\sigma\sqrt{2\pi}} \cdot e^{\frac{-d^2}{2\sigma^2}} \quad (9)$$

where $\sigma$ is proportional to the edge length and $d$ is the distance between the phonon's position and the vertex $v_i$. Furthermore we consider only phonons $ph_k$ which satisfy the condition shown in the equation below:

$$\langle n_t, n_{v_i}\rangle > 0 \quad (10)$$

Here $n_t$ is the normal of the triangle containing the phonon $ph_k$ and $n_{v_i}$ denotes the normal at $v_i$. The latter can be calculated as interpolation normal of the corresponding triangle normals. The second approach which we utilize to calculate the importance of the vertices takes only phonons $ph_k$ into account which are located in a tight neighborhood of $v_i$. This means the distance of the phonon's position to the considered vertex is smaller than a given threshold. The importance value of $v_i$ is then the average of the importance values $imp(ph_k)$ of the phonons $ph_k$:

$$imp_{v_i} = \frac{\sum_{k=0}^{m} imp(ph_k)}{m} \quad (11)$$

Additionally, the condition in 10 have to be satisfied for two-sided scene elements.

Now, since we have calculated the importance values for each vertex in the scene we assign color to each $v_i$ according to these values. The color value for $v_i$ is calculated as follows:

$$c_{v_i} = \alpha \cdot hue_{max} + (1.0-\alpha)\cdot hue_{min}$$
$$\alpha = \frac{imp_{v_i} - imp_{min}}{imp_{max} - imp_{min}} \quad (12)$$

where $imp_{min}$ and $imp_{max}$ are the minimum and maximum importance values in the scene and $hue_{min}$ and $hue_{max}$ denote the minimum and maximum hue values, respectively. We choose red color for $hue_{max}$ and blue color for $hue_{min}$ and interpolate the color for the vertices $v_i$ from red to blue in HSV color space. Since we now have the refined triangulated geometry of considered scene, and color values for each $v_i$ corresponding to the importance values we can render the entire scene using OpenGL texture mapping techniques or simple primitives rendering.

Furthermore, our visualization system provides some additional options for user interaction:

- selection of break-off time $t_{end}$ for early reflections
- selection of start time $t_{start}$ for late reflections
- selection of one listener position $l_i$
- selection of one object $o_j$ inside the scene

## 6 Results

In the following we present the results of our listener-based analysis of surface importance for acoustic metrics presented above. We apply the method to the acoustic improvement of a lecture hall at the university. A main acoustic measure for a lecture hall is the comprehensibility of speech which is expressed with the acoustic metric clarity ($C_{50}$). The $C_{50}$ values alone only show the current acoustic state but give no insight how it can be improved (i.e. where to put absorbing material). The listener-based analysis of surface importance overcomes this drawback by visualizing the directional aspect by means of mapping importance values to the room surfaces. In the case of clarity the importance is based on energy received in the first $50ms$ after the primary wave front and energy received after the first $50ms$, respectively. The visualization of these importance values give a clear advice which parts of the room geometry need to be changed (by means of exchanging material) to improve the chosen acoustic metric (clarity).

To assess the value of our visualization we use glyphs which represent the $C_{50}$ value at different listener positions. The $C_{50}$ values are derived from simulated impulse responses for each position.

Since we are looking at the comprehensibility of the human speech, which has a frequency range from 150 Hz - 4 kHz with a main focus around 1kHz [9], we use the 1 kHz octave band for our evaluation. For the improvement of a music hall, one has to adjust and use more octave bands because music spans a wider range of frequencies than human speech.

### 6.1 Glyphs

Like mentioned before, the ratio between the early reflections and late reverberations is important for example for the comprehensibility of speech, which itself is significant for planning a lecture room. In order to visualize this metric (clarity $C_{50}$) we use glyphs analog to the approach described in [24]. The representation of the glyphs is as follows. The early reflections and late reverberations are represented as semicircles where the semicircle for the early reflections is placed above that for late reverberations. The radii of the semicircles correspond to the early and late received energy, respectively. Thus, the direct comparison of early and late reflections is possible. Additionally to the ratio the glyphs also show if the clarity is above a certain threshold (i.e. $C_{50} > 3dB$). This is visualized by coloring the lower semicircle green for above or red for below the chosen threshold respectively. This is depicted in figure 5.

Nevertheless, this metric is independent from the direction of the arriving sound wave at a listener position and gives only insight in the current acoustic state. We apply the clarity visualization using the glyphs for evaluation of our listener-based importance visualization.

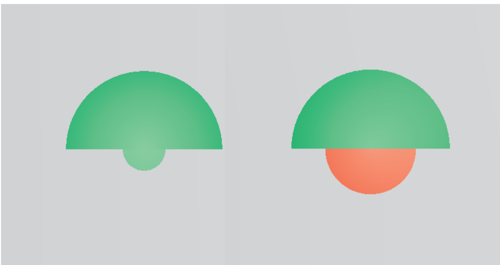

Fig. 5. Example for clarity ($C_{50}$) visualization using glyphs. Left: $C_{50}$ above given threshhold (green lower semicircle). Right: $C_{50}$ below given threshhold (red lower semicircle).

### 6.2 Lecture Hall

The university lecture hall subject to acoustic optimization is presented in figure 6. The materials used in this hall are as follows:

- concrete (floor, ceiling, gray walls)
- metal (doors, blackboard frame)
- wood (desk, benches, brown walls)

Speaker and audience are depicted by the green and blue spheres, respectively. We used the simulation algorithm described in section 3 to calculate the impulse response and thus the definition and clarity values at the listener positions. An example of the sound particle propagation inside the lecture hall is given in figure 1. To get an overview of the current acoustic state of the room we visualize the above described glyphs for the clarity ($C_{50}$) measure at all listener positions. Because we want to improve the comprehensibility of speech the $C_{50}$ values for the 1kHz frequency band are shown in figure 7 (a). These values are derived from the impulse responses at the different listener positions. For the simulation of the impulse responses the actual material/absorption coefficients were used. The threshold for $C_{50}$ was set to $3dB$.

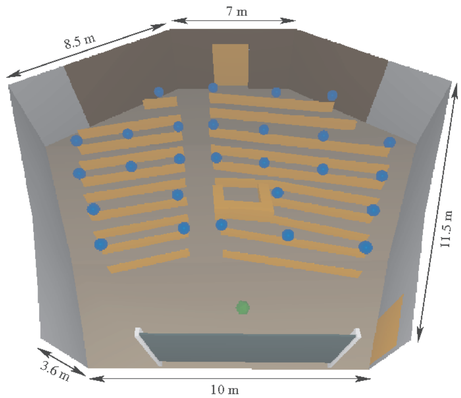


Fig. 6. Lecture Room setup. Green: speaker, blue: audience

Figure 7 (a) clearly shows that the desired clarity is only reached at the three closest positions to the speaker (green lower semicircles of the glyphs). Depending on the individual hearing ability of the listeners the second and third row could be acceptable (red lower semicircle but smaller than upper green semicircle) whereas the clarity in the last two rows is unacceptable (red semicircle is bigger than green semicircle). This clearly indicates the need of acoustic improvement, but the glyphs cannot give any cue how to alter the room so that the acoustic situation is acceptable.

### 6.3 Analysis of Surface Importance

To get insight into the directional aspect of the current acoustic situation we calculate importance values based on the chosen acoustic metric (clarity $C_{50}$). As clarity describes the ratio between early ($< 50ms$) and late ($> 50ms$) received energy we chose the break-off time $t_{off} = 50ms$ for early and the start time $t_{start} = 50ms$ for late reflections. All values were calculated for the 1kHz frequency band with all listener positions taken into account. The importance values are then mapped to the room surfaces as shown in figures 8 (a) + (b) (topview) and 9 (a) + (b) (sideview). In addition to the importance for early and late reflections we calculate a difference image by subtracting the importance for early reflections from the importance for late reflections (figures 8 (c) + 9 (c))

As described in section 5 the highest importance value $imp_{max}$ is mapped to $hue_{max}$ (red) and the lowest importance value $imp_{min}$ to $hue_{min}$ (blue). Thus red areas in figures 8 (a) + (b) and 9 (a) + (b) depict the parts of the room surface which contribute most to early (a) and late (b) reflections.

In figures 8 (c) and 9 (c) red areas depict parts of the geometry which are important for late reflections but unimportant for early reflections and blue vice versa. Light green areas are equally important for early and late reflections. Thus the absorption coefficients of the surfaces in the red areas can be changed to alter the amount of late received energy without a large effect on the amount of early received energy and vice versa.

To enhance the $C_{50}$ values throughout the lecture hall it is necessary to reduce the amount of late received energy at the listener positions. The visualization of the surface importance for early and late reflections gives a direct cue how to improve the overall clarity in the given room by simple changes. When looking at figures 8 (b) and 9 (b) one can directly locate the most important surfaces for late reflections which are the sidewalls of the room (red). An inspection of the difference images (figures 8 + 9 (c)) indicates that the change of the back wall material will not influence the early reflections too much (also red color of the back wall). Therefore we exchanged the material of the back wall (wood) with highly absorbing material (sound absorbing foam) to reduce the late reflections throughout the audience without cutting out the early reflections.

To evaluate our changes we simulate the impulse responses for the listener positions and recalculate the $C_{50}$ values according to the new material/absorption coefficients. Figure 7 (c) shows the improvement in clarity at the listener positions throughout the audience. The $C_{50}$ values for almost all listener positions exceed the chosen threshold (green lower semicircles). We now have to take a closer look at the two positions which did not satisfy the desired threshold (marked as $A$ and $B$ in figure 7 (c)).

Figures 10 and 11 (a)-(c) show the importance values when only the single listener positions $A$ and not the whole audience is taken into account (importance for (a) early and (b) late reflections, difference image (c)). From figure 10 it is directly apparent that the change of the back wall material only has a medium impact on the clarity for listener position $A$. The main contribution to the late received energy is received from the rightmost corner of the room (which was not changed) rather than from the back wall. Thus if we want to enhance the clarity for listener position $A$ only and not for the whole audience we need to change the material in the red areas in figure 10 (c). When looking at figures 11 (a)-(c) (importance for listener position $B$) we can see a problem which occurs when we take the whole audience into account. While the back wall is important for late reflections but nearly unimportant for early reflections to the whole audience, it is important for early and late reflections when taking only listener position $B$ into account. The exchange of the back wall material resulted in a decrease of late reflections to this position (which was intended) but also reduced the amount of early reflections. Thus the clarity (depending on the early to late reflection ratio) only improves slightly compared to the rest of the audience. To improve the clarity at this single position it would be most effective to alter the absorption of the floor material (red area in figure 11 (c)) for example exchanging the flooring material but the impact on the whole audience would not be as good as the conducted changes to the back wall.

For evaluation purposes we also exchanged the material of a surface (ceiling above speaker) which is on the one hand only medium important for late reflections and on the other hand also has some influence on the early reflections. The resulting $C_{50}$ glyphs are visualized in figure 7 (b). As expected the improvement in clarity is only partial because the chosen surface is only medium important for late reflections taking the whole audience into account, whereas it is more important for the listeners in the first two rows ($C_{50}$ reaches the desired threshold, i.e. green lower semicircles).

Overall the listener-based analysis of surface importance proves to be a useful tool to understand application specific data and to get insight into the directional aspect of the acoustic situation in a room for a certain acoustic metric which is not apparent when looking at the resulting values only. Through the visualization of surface importances for a certain metric we could easily locate the parts of the room surface which affect this metric the most. Thus we were able to improve the current acoustic situation with selective changes to the most important surfaces of the room.

## 7 Conclusions

We have presented an approach for the listener-based analysis of surface importance relative to an acoustic metric. By calculating importance values for the whole room geometry based on a chosen acoustic metric and the listener positions we were able to get a deeper insight into the current acoustic situation of the room, especially the directional aspect. This insight could not be obtained with simpler approaches (like looking at only the first reflection). With this additional information which is not apparent from the acoustic metric itself we were able to locate the parts of the room surface which need to be changed to efficiently improve the chosen metric.

We have discussed an application scenario of our visualization where we have analyzed and improved the acoustic situation inside a lecture room at the university considering the comprehensibility of speech, measured by the clarity ($C_{50}$) metric. Of course, our approach can easily be extended to consider other acoustic metrics which can be derived from the room impulse response. For the calculation of the impulse responses at given listener positions we used a sound particle tracing approach.

Considering automatic optimization methods, the introduced approach is a first step towards the solution of an inversion problem optimizing the room geometry and/or material properties to achieve appropriate quality of an existing or planned room. By means of well defined acoustic metrics it can be evaluated if a room is suitable for speech or music presentations. The challenge for the mentioned inversion problem is to find an appropriate formal description which concludes how the room shape influences the given metric to be able to start optimization algorithms for room improvement.

## Acknowledgements

We thank the members of the Visualization and Computer Graphics Research Groups at the University of Kaiserslautern and the members of the International Research Training Group (IRTG 1131). The IRTG 1131 is supported by the German Research Foundation (DFG). This work was supported by the Rheinland Pfalz Cluster of Excellence on Dependable and Adaptive Systems and Mathematical Modeling (DASMOD).

## References


[1] *DIN EN ISO 3382:2000-03*.

[2] *Formulas of Acoustics*. Springer Publishers, 2002.

[3] J. Allen and A. Berkeley. Image method for efficiently simulating small-room acoustics. *J. Acoust. So. Amer.*, 65(4):943–950, 1979.

[4] F. Antonacci, M. Foco, A. Sarti, and S. Tubaro. Fast modeling of acoustic reflections and diffraction in complex environments using visibility diagrams. In *Proceedings of the 12th European Signal Processing Conference (EUSIPCO 04)*, pages 1773–1776, Vienna, Austria, September 2004.

[5] M. Bertram, E. Deines, J. Mohring, J. Jegorovs, and H. Hagen. Phonon tracing for auralization and visualization of sound. In *IEEE Visualization*, pages 151–158, Minneapolis, MN, October 2005.

[6] J. Borish. Extension of the image model to arbitrary polyhedra. *J. Acoust. So. Amer.*, 75(6):1827–1836, 1984.

[7] Bose Corporation. Bose modeler. *http://www.bose.com*.

[8] CATT. Catt-acoustic. *http://www.catt.se*.

[9] L. Cremer. *Principles and Applications of Room Acoustics: Geometrical, Statistical and Psychological Room Acoustics*. Chapman & Hall, 1982.

[10] E. Deines, M. Bertram, J. Mohring, J. Jegorovs, F. Michel, H. Hagen, and G. M. Nielson. Comparative visualization for wave-based and geometric acoustics. In *Transactions on Visualization and Computer Graphics (TVCG), Proceedings of IEEE Visualization*, volume 12, pages 1173–1180, 2006.

[11] E. Deines, F. Michel, M. Bertram, H. Hagen, and G. M. Nielson. Visualizing the phonon map. In *Proceedings of EuroVis*, pages 291–298, Lisboa, 2006.

[12] T. A. Funkhouser, I. Carlbom, G. Elko, G. P. M. Sondhi, and J. West. A beam tracing approach to acoustic modeling for interactive virtual environments. In *Computer Graphics (SIGGRAPH 98)*, pages 21–32, Orlando, FL, July 1998.

[13] T. A. Funkhouser, P. Min, and I. Carlbom. Real-time acoustic modeling for distributed virtual environments. In *Computer Graphics (SIGGRAPH 99)*, pages 365–374, Los Angeles, August 1999.

[14] H. W. Jensen. Global illumination using photon maps. In *Rendering Techniques '96 (Proceedings of the 7th Eurographics Workshop on Rendering)*, pages 21–30, 1996.

[15] B. Kapralos, M. Jenkin, and E. Milios. Acoustical diffraction modeling utilizing the huygens-fresnel principle. In *Proceedings of the IEEE HAVE 2005*, page 6 pp., Ottawa, Ontario, Canada, 2005.

[16] B. Kapralos, M. Jenkin, and E. Milios. Acoustical diffraction modeling for interactive virtual environments. In *Proceedings of the 2nd International Conference on Computer Graphics Theory and Applications (GRAPP 2007)*, Barcelona, Spain, March 8-11 2007.

[17] B. Kapralos, M. Jenkin, and E. Millios. Sonel mapping: Acoustic modeling utilizing an acoustic version of photon mapping. In *IEEE International Workshop on Haptics Audio Visual Environments and their Applications (HAVE 2004)*, pages 1–6, Ottawa, Canada, October 2-3 2004.

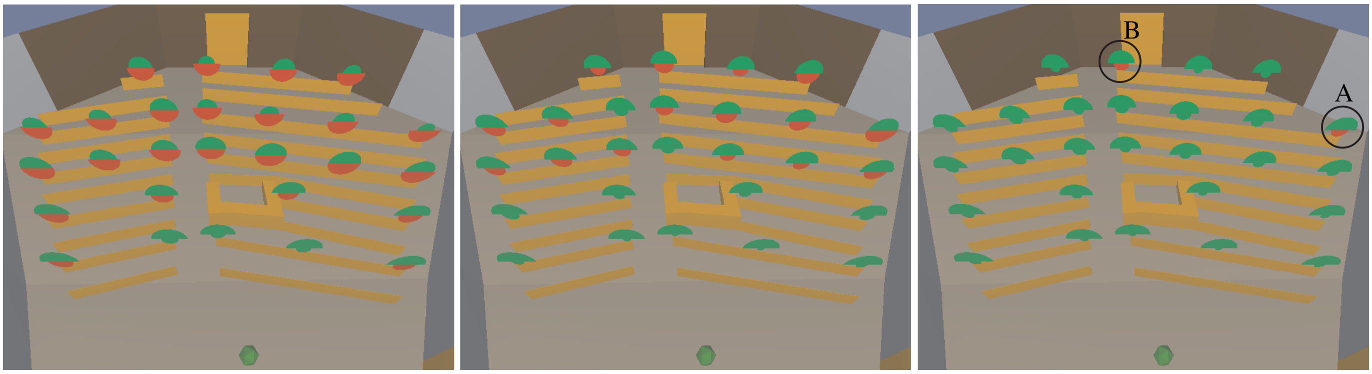


(a) (b) (c)

Fig. 7. $C_{50}$ Glyphs at listener positions in the lecture hall. (a) Actual materials/absorption coefficients. (b) Glyphs at listener positions for changed ceiling (above speaker) material with highly absorbing material (sound absorbing foam). (c) Glyphs at listener positions for changed backwall material with sound absorbing foam.

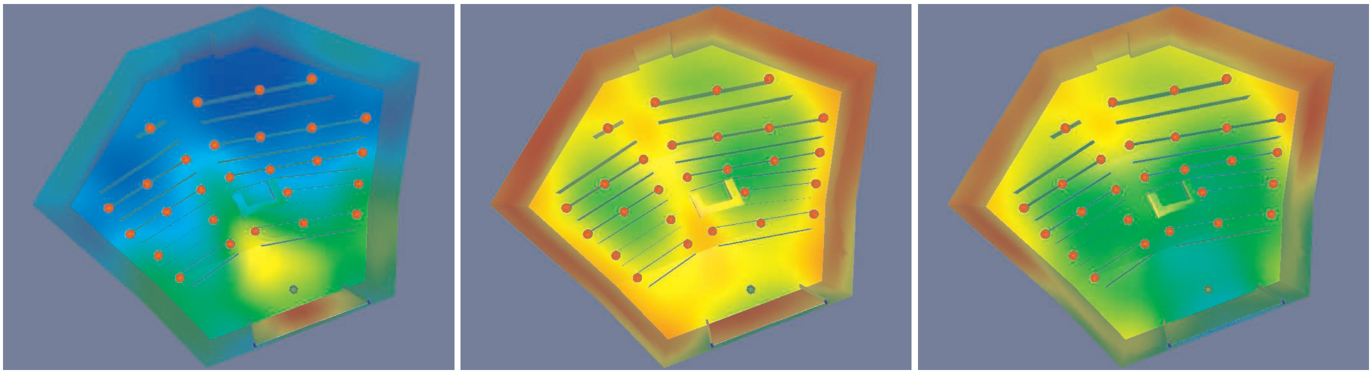

(a) (b) (c)

Fig. 8. Importance values whole audience and 1kHz mapped to the room surfaces (topview). (a) Importance for early reflections ($< 50ms$), (b) Importance for late reflections ($> 50ms$) red: highest importance, blue: unimportant. (c) Difference (importance for late reflections - importance for early reflections) red: only important for late reflections blue: only important for early reflections.

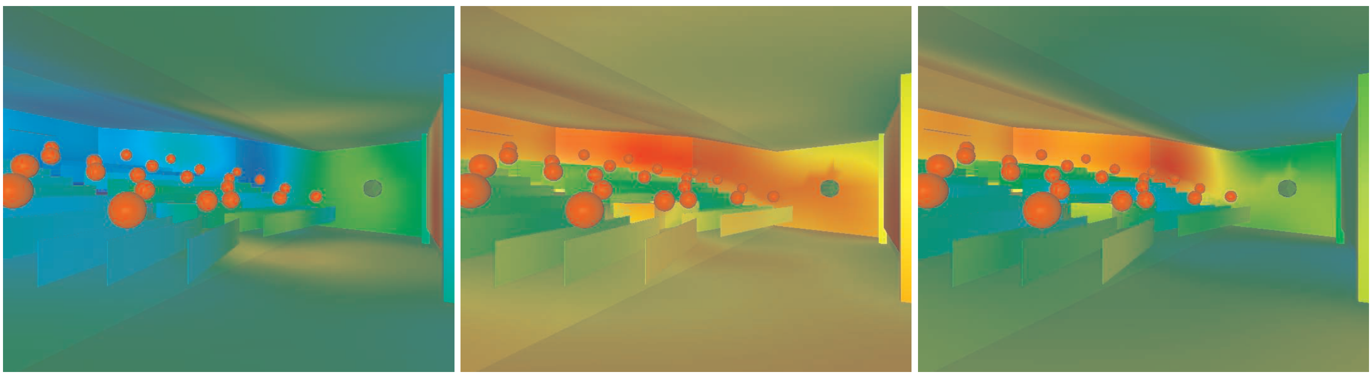

(a) (b) (c)

Fig. 9. Same as figure 8 from side view.

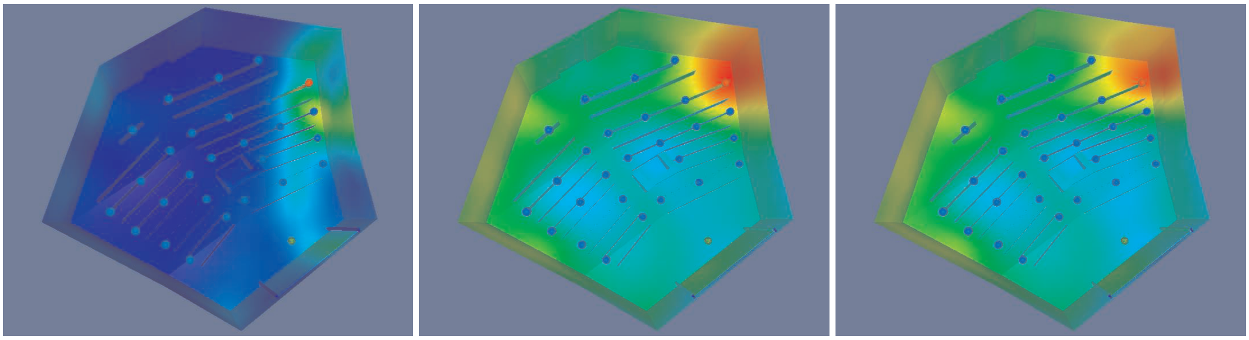

(a) (b) (c)

Fig. 10. Importance values for listener position $A$ and 1kHz mapped to the room surfaces (a) Importance for early reflections. (b) Importance for late reflections. (c) Difference. (Same as figure 8 for single listener).

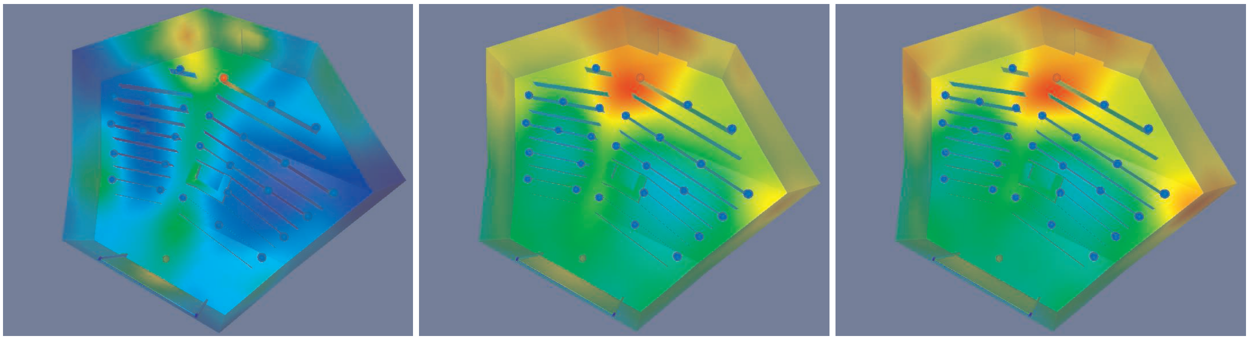

(a) (b) (c)

Fig. 11. Same as figure 10 for listener position $B$.


[18] S. Khoury, A. Freed, and D. Wessel. Volumetric visualization of acoustic fields in cnmat's sound spatialization theatre. In *Visualization '98*, pages 439–442 & 562. IEEE, 1998.

[19] U. Krockstadt. Calculating the acoustical room response by the use of a ray tracing technique. *Journal of Sound and Vibrations*, 8(18), 1968.

[20] U. Kulowski. Algorithmic representation of the ray tracing technique. *Applied Acoustics*, 18:449–469, 1984.

[21] M. Monks, B. Oh, and J. Dorsey. Acoustic simulation and visualization using a new unified beam tracing and image source approach. In *Convention of the Audio Engineering Society*. ACM, 1996.

[22] ODEON. Room acoustic software. *http://www.odeon.dk*.

[23] D. Schröder. Image sources audibility test for real-time applications using binary space partitioning. In *Proceedings of the POSTER 2005 conference*, Prague, Czech Republic, 2005.

[24] A. Stettner and D. Greenberg. Computer graphics visualization for acoustic simulation. In *International Conference on Computer Graphics and Interactive Techniques*, pages 195–206. ACM, 1989.

[25] N. Tsingos, T. Funkhouser, A. Ngan, and I. Carlbom. Modeling acoustics in virtual enviroments using the uniform theory of diffraction. In *28th Annual Conference on Computer Graphics nad Interactive Techniques (SIGGRAPH 01)*, pages 545–552, Los Angeles, August 2001.

[26] M. Vorländer. Simulation of the transient and steady-state sound propagation in rooms using a new combined ray-tracing/image-source algorithm. *J. Acoust. So. Amer.*, 86(1):172–178, 1989.